Journal Pre-proof

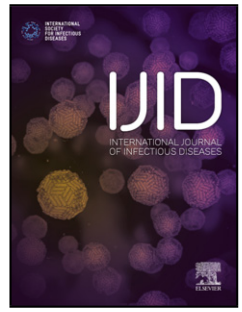


High-resolution Chest CT Features and Clinical Characteristics of Patients Infected with COVID-19 in Jiangsu, China

Hui Dai Xin Zhang Jianguo Xia Tao Zhang Yalei Shang Renjun Huang Rongrong Liu Dan Wang Min Li Jinping Wu Qiuzhen Xu Yonggang Li

PII: S1201-9712(20)30218-6

DOI: https://doi.org/doi:10.1016/j.ijid.2020.04.003

Reference: IJID 4091

To appear in: *International Journal of Infectious Diseases*

Received Date: 26 February 2020

Revised Date: 30 March 2020

Accepted Date: 1 April 2020

Please cite this article as: Dai H, Zhang X, Xia J, Zhang T, Shang Y, Huang R, Liu R, Wang D, Li M, Wu J, Xu Q, Li Y, High-resolution Chest CT Features and Clinical Characteristics of Patients Infected with COVID-19 in Jiangsu, China, *International Journal of Infectious Diseases* (2020), doi: https://doi.org/10.1016/j.ijid.2020.04.003

**Title:** High-resolution Chest CT Features and Clinical Characteristics of Patients Infected with COVID-19 in Jiangsu, China

**Author list**

Hui Dai[#a,b], Xin Zhang[#c], Jianguo Xia[d], Tao Zhang[e], Yalei Shang[a], Renjun Huang[a], Rongrong Liu[f], Dan Wang[g], Min Li[*f], Jinping Wu[*g], Qiuzhen Xu[*h], Yonggang Li[*a,b]

[a] Department of Radiology, the First Affiliated Hospital of Soochow University, Suzhou city, Jiangsu province, P.R.China 215000

[b] Institute of Medical Imaging, Soochow University, Suzhou city, Jiangsu province, P.R.China 215000

[c] Department of Radiology, the Fourth People's Hospital of Huaian, Huai'an city, Jiangsu province, P.R.China 223001

[d] Department of Radiology, Taizhou People's Hospital, Hospital Affiliated 5 to Nantong University, Taizhou city, Jiangsu province, P.R.China 225300

[e] Department of Radiology, the Third Hospital Affiliated of Nantong University, Nantong City, Jiangsu province, P.R.China 226000

[f] Department of Radiology, The Affiliated Infectious Diseases Hospital of Soochow University, Suzhou city, Jiangsu province, P.R.China 215000

[g] Department of Radiology, the Third People's Hospital of Changzhou, Changzhou city, Jiangsu province, P.R.China 213000

[h] Department of Radiology, Zhongda Hospital Affiliated to Southeast University, Nanjing city,

Jiangsu province, P.R.China 210000

[#] These authors contributed equally to this work.

* Corresponding Author

**Corresponding Author 1**

Yonggang Li Ph.D.

e-mail: liyonggang224@163.com

telephone number: 0086-512-67780155

fax number: 0086-512-65228072

correspondence address: Department of Radiology, the First Affiliated Hospital of Soochow University, Suzhou, Jiangsu, P.R.China 215000

**Corresponding Author 2**

Min Li M.D.

e-mail: 105549156@qq.com

telephone number: 0086-512-67780633

fax number: 0086-512-67780633

correspondence address: Department of Radiology, The Affiliated Infectious Diseases Hospital of Soochow University, Suzhou city, Jiangsu province, P.R.China 215000

**Corresponding Author 3**

Jinping Wu M.D.

e-mail: czwjp@sina.com

telephone number: 0086-519-82009212

fax number: 0086-519-82009212

correspondence address: Department of Radiology, the Third People Hospital of Changzhou, Changzhou city, Jiangsu province, P.R.China 213000

**Corresponding Author 4**

Qiuzhen Xu M.D.

e-mail: xuqiuzhen831@sina.com

correspondence address: Department of Radiology, Zhongda Hospital Affiliated to Southeast University, Nanjing city, Jiangsu province, P.R.China 210000

## ABSTRACT

**Background**

A pneumonia associated with the coronavirus disease 2019 (COVID-19) recently emerged in China. It was recognized as a global health hazard.

**Methods**

234 inpatients with COVID-19 were included. Detailed clinical data, chest HRCT basic performances and certain signs were recorded, and ground-glass opacity (GGO), consolidation, fibrosis and air trapping were quantified. Both clinical types and CT stages were evaluated.

**Results**

Most patients (approximately 90%) were classified as common type and with epidemiologic history. Fever and cough were main symptoms. Chest CT showed abnormal attenuation in bilateral multiple lung lobes, distributed in the lower and/or periphery of the lungs (94.98%), with multiple shapes. GGO and vascular enhancement sign were most frequent seen, followed by interlobular septal thickening and air bronchus sign as well as consolidation, fibrosis and air trapping. There were significant differences in most of CT signs between different stage groups. The SpO2 and OI were decreased in stage IV, and the CT score of consolidation, fibrosis and air trapping was significantly lower in stage I ($P < 0.05$). A weak relevance was between the fibrosis score and the value of PaO2 and SpO2 ($P < 0.05$).

**Conclusions**

Clinical performances of patients with COVID-19, mostly with epidemiologic history and typical symptoms, were critical valuable in the diagnosis of the COVID-19. While chest HRCT provided the distribution, shape, attenuation and extent of lung lesions, as well as some typical CT signs of

COVID-19 pneumonia.

**Keywords** SARS-CoV-2, COVID-19, High-resolution CT (HRCT)

## Introduction

In December 2019, an outbreak of pneumonia of unknown etiology was reported in Wuhan, Hubei province, China. The Chinese Center for Disease Control and Prevention (CDC) isolated the causative viral pathogen from throat swabs sample of the affected patients. The pathogen was a novel coronavirus named severe acute respiratory syndrome coronavirus 2 (SARS-CoV-2) by WHO and the disease caused by SARS-CoV-2 was termed as coronavirus disease 2019 (COVID-19). Up to February 18, 2020, 58097 laboratory-confirmed cases of COVID-19 and 1870 deaths have been reported in China, posing great threats to global public health.

SARS-CoV-2, severe acute respiratory syndrome coronavirus (SARS-CoV) and the Middle East respiratory syndrome coronavirus (MERS-CoV)[1][2][3] are subgroups of betacoronavirus genus. As far as we known, the symptoms of COVID-19 range from mild to severe. They can be fever, dry cough, shortness of breath, and in some severe cases, kidney failure or death similar to SARS-CoV infection may occur[4]. However, information regarding to the radiological and clinical features of the pneumonia associated with COVID-19 is still scarce, making it difficult for physicians to distinguish the causative agents without genetic related laboratory analysis. Moreover, reverse transcription-polymerase chain reaction (RT-PCR), the gold standard for a confirmative diagnosis of COVID-19, has obvious limitations, such as certain proportion of false negative results, limited sampling method and shortage of kits. Computed tomography (CT) of the chest is increasingly recognized as strong evidence for early diagnosis, because the changes in chest imaging sometimes maybe earlier than clinical symptoms. Considering that fewer confirmed cases were included in previous studies[5], we set up a Jiangsu multi-center study, to collect a considerable larger sample size in this retrospective study. The purpose of the study is to improve the comprehension of the newly-emerged diseases in order to make the diagnosis earlier, by describing the comprehensive chest CT characteristics and clinical features of patients with COVID-19, who were admitted to the designated hospitals in Jiangsu province, China.

## METHODS

### Patients and clinical data

This study was conducted in accordance with the amended Declaration of Helsinki. Independent ethics committees approved the protocol, and written informed consent was obtained from all patients. This was a multi-centered study included 234 inpatients from 13 hospitals during 17 days (from January 10th to February 7th 2020) in Jiangsu. All the cases were confirmed with the criteria for SARS-CoV-2 infection established by National Health Commission, which was consistent with one of the following two conditions, based on the pathogenic evidence: 1) positive in real-time fluorescent RT-PCR detection of novel coronavirus nucleic acid in specimens from respiratory tract or blood; 2) virus was highly homologous to the known novel coronavirus in genetic sequencing analyses in specimens from respiratory tract or blood. All the cases underwent an additional microbiological evaluation for ruling out other suspected respiratory infections. Those with a proved additional concurrent acute illness or other preexisting medical conditions were also excluded.

Clinical data were recorded, containing age, gender, occupation, epidemic history and disease severity. Present history, symptoms and signs, blood routine outcomes and therapeutic schedules were also recorded. There were four clinical types according to the severity of disease -- mild type, subtle or mild clinical symptoms and no pneumonia found on CT images; common type, fever or respiratory symptoms, etc. and pneumonia observed on CT images; severe type, fulfil any one of the following conditions 1) respiratory distress, respiratory rate (RR) ≥30 times per minute, 2) resting state oxygen saturation (SpO2) ≤93%, or 3) oxygenation index (OI) (calculated by partial pressure of oxygen (PaO2)/fraction of inspired oxygen (FiO2)) ≤300mmHg (1mmHg=0.133kPa); critical severe type, fulfil any one of the following conditions 1) respiratory failure and mechanical ventilation needed, 2) shock, 3) combined failure of other organ and ICU monitoring and treatment needed.

**CT scanning**

Each subject underwent chest high-resolution CT (HRCT) examination within 24 hours after admission. Inspiratory phase of chest HRCT examination was performed during a single-breath hold at full inspiration. The CT scanner models from the hospitals involved in this multicenter study were listed as following: GE Bright Speed Elite 16, Neusoft 16, SOMATOM Emotion, SOMATOM definition AS, PHLIPS MX-16, Philips 64-row spiral Ingenuity and the UNITED IMAGING Elite 16. The scanning parameters were as following: tube voltage 120kV, tube current 110mA, pitch 1.0, rotation time ranging from 0.5s to 0.75s, slice thickness 5mm, with 1mm or 1.5mm section thickness for axial, coronal and sagittal reconstructions.

**CT evaluation**

Two experienced attending radiologists, blinded to the clinical information, separately reviewed and scored the CT images. The expert group, containing 3 senior radiologists with working experience more than 10 years, would make the final decision if there is a divergent opinion between the two attending.

1. Basic CT performances

The distribution features and the shape of abnormal attenuation, as well as the involved lung lobes, were recorded. If there were any common accompanying diseases of lung, such as obsolete pulmonary tuberculosis, emphysema, bronchiectasia, tumor and others, they would be recorded.

2. Certain CT signs

The following CT performances were judged and recorded as 0 or 1 (0 for none, 1 for yes), including vascular enhancement sign (VES, vascular enlargement inside the lesion resulted from congestion and dilation of small vessels), air bronchus sign, reticular/mosaic sign (defined as a collection of innumerable small linear opacities that, by summation, produced an appearance resembling a net[6]), bronchial wall thickening, interlobular septal thickening, interlobar fissure displacement, solid nodules, intralesional and/or perilesional bronchiectasis, mediastinal lymphadenopathy, pleural effusion, pleural thickening and pericardial effusion.

3. Quantified evaluation

The signs of ground-glass opacity (GGO), consolidation, fibrosis and air trapping and were analyzed quantitatively using a radiologic scoring system ranging from 0-25 points, which was an adaptation of the method previously used to describe idiopathic pulmonary fibrosis and SARS[7]. Each lung lobe was evaluated by 0-5 points, on the basis of the area involved, with score 0 for normal performance, 1 for less than 5% of lung lobe areas involved, 2 for 6%–25%, 3 for 26%–50%, 4 for 51%–75%, and 5 for more than 75%. A total score was eventually recorded via the addition of the score of each lobe.

4. CT stages

According to the performances of CT images, the cases were classified into four stages – stage I (early stage), stage II (progressive stage), stage III (recovery stage), and stage IV (severe stage). The classification method was mainly according to the following CT performances. Stage I: single or multiple lesions, in irregular, round-like or patchy shapes, generally not involved the whole lung segment, often showed GGO with vascular enlargement. Stage II: more extensive lesions, involved bilateral multiple lobes predominantly in the sub-pleural areas, in irregular, round-like, patchy and "anti-butterfly" shapes, scattered or diffused patches even fusing into large patches with density increased, often with vascular enlargement, reticular sign and bronchial wall thickening, occasionally with less fibrosis and sub-segment atelectasis. Stage III: the lesions absorbed and diminished, the focus can be completely absorbed, with residual fiber stripes. Stage IV: bilateral diffuse lesions, more than half of the lung field involved, even extended to the whole lung and presented as "white lung".

**Statistical analysis**

The statistical analyses were performed by Statistical Product and Service Software (SPSS ver. 26.0, Chicago, IL, USA). Descriptive statistics was used in clinical data and some basic information of CT images. Pearson Chi-square test and Fisher exact probability test were used in dichotomous variables (0 or 1) to test the differences of these variables among different CT stages groups. Kruskal–Wallis H test was used to test the group differences of multiple quantitative variables (arterial blood gas (ABG) analysis results and CT scoring). Spearman rank correlation was used to measure the degree of association between the arterial blood gas (ABG) analysis results and CT scoring. A P value less than 0.05 was considered statistically significant and

Bonferroni correction was used to adjust P values in multiple comparisons. The mean values were showed as MEAN±SE.

**Results**

**Clinical data**

234 patients infected with SARS-CoV-2 confirmed by real time RT-PCR were included in this study, among which 6 patients were with initial RT-PCR negative and follow-up test positive. There were 136 (58.1%) men and 98 (41.9%) women, with average age (44.6±14.8) years old (ranging from 7 to 82 years old). The age and occupation distribution of the patients were showed in Table-1. Stuff was the most frequency occupation (46.2%) in this study. Approximately 90% patients had epidemiologic linkage to Hubei Province or closely contacted with other confirmed cases and almost 90% patients were classified as common type, as showed in Table-1.

Fever (72.6%) and cough (64.1%) were main symptoms of patients infected with SARS-CoV-2. There were some other symptoms such as pharyngeal discomfort (15%), fatigue (13.2%), chill (9.8%), muscle ache (9.0%), rhinobyon and snivel (5.6%), diarrhea (3.8%), chest pain (3.4%), chest tightness (5.6%), short of breath (2.1%), difficulty breathing (3%) and nausea and vomiting (2.1%). Most of patients were with normal range of leukocytes count, neutrophils count, lymphocytes count, neutrophil ratio and lymphocyte ratio in the first blood routine examination during hospitalization. The proportion of normal cases were respectively occupied 75.1%, 81.7%, 82.6% and 59.7% of all the patients. As to the therapy schedules, each patient was received an antiviral therapy (oral or intravenous antiviral drugs, and inhalation of interferon). Antibiotics was administered in 118 (50.4%) patients to prevent or treat concomitant bacterial infection, methylprednisolone in 34 (14.5%) to suppress the inflammatory response, gamma globulin in 34 (14.5%) to boost immunity, and non-invasive ventilator was used in 11 (4.7%) cases (severe or critical severe patients).

**Chest CT analysis**

1. Basic CT performances and CT stages

15 (6.4%) patients were without abnormal lung changes by Chest HRCT examination, hence the CT images of 219 patients were analyzed. 192 cases were with bilateral multiple lung lobes involved (87.67%, 192/219), of which 121 cases (63.02%, 121/192) were involved with whole lung. Merely 16 cases (7.31%, 16/219) were involved with single lobe. 208 cases (94.98%, 208/219) were mainly distributed in the lower lungs and/or the periphery of the lungs. The shape of the lesions was mainly irregular (88.13%, 193/219), followed by small patches (86.3%, 189/219), strip-like (69.41%, 152/219), round-like (49.32%, 108/219) and “anti-butterfly” (47.95%, 105/219). 60 patients (27.4%, 60/219) were with common accompanying diseases of lung, of which emphysema (including localized emphysema) and bullae was the most common (88.33%, 53/60), followed by bronchiectasia (16.67%, 10/60).

According to the performance of chest CT, the patients were divided into stage I-IV, as the cases showed in Figure-1, Figure-2, Figure-3 and Figure-4. 80 cases (36.53%, 80/219) were classified into stage I group, 86 cases (39.27%, 86/219) into stage II group, 43 cases (24.2%, 43/219) into stage III group and 10 cases (4.57%, 10/ 219) into stage IV.

2. Certain CT signs

Among the 219 patients with positive chest HRCT performances, 207 cases were with VES, 205 with interlobular septal thickening, 184 with air bronchus sign, 173 with intralesional and/or perilesional bronchiectasis, 170 with pleural thickening, 138 with solid nodules, 135 with reticular/mosaic sign, 124 with interlobar fissure displacement, 76 with bronchial wall thickening, 29 with minor pleural effusion and pericardial effusion, 21 with mediastinal lymphadenopathy.

The frequency of VES was the highest, but there was no significant difference among the four stage groups, as showed in Table-2. The frequency of interlobular septal thickening, air bronchus sign and intralesional and/or perilesional bronchiectasis in stage I was significantly lower than that in stage II and stage III ($P < 0.008$). The frequency of reticular sign, pleural thickening and interlobar fissure displacement was the lowest in stage I ($P < 0.008$). The frequency of solid nodules in stage IV was significantly higher than that in stage 1 ($P < 0.008$). The frequency of bronchial wall thickening was lower in stage I than that in stage III and stage IV ($P < 0.008$).

The frequency of pleural effusion, pericardial effusion and mediastinal lymphadenopathy was relatively small. The frequency of pleural effusion was lower in stage I than that in stage III and stage IV, and it was also lower in stage II than that in stage IV ($P < 0.008$). The frequency of mediastinal lymphadenopathy was lower in stage I than that in stage III ($P < 0.008$). There was no significant difference of the frequency of pericardial effusion among the four groups.

**Analysis about clinical and CT quantified data**

1. Multiple comparisons among stage I-IV groups

As to the group differences of indices from ABG analysis, the $SpO_2$ ((94.70±0.20)%) of patients in stage IV group was significantly lower than that ((97.2±0.91)%) in stage II group, and the OI ((200.25±24.75) mmHg) of patients in stage IV was lower than that ((470.71±38.81) mmHg) in stage I ($P < 0.05$) (Table-3). There were no significant differences of RR and $PaO_2$ among stage I-IV groups ($P > 0.05$).

As to the group differences of CT scores, the CT score of consolidation (5.71±0.42) in stage I was significantly lower than those in other three groups (respectively 7.06±0.49, 7.60±0.66, 8.30±1.72), and the CT score of fibrosis (1.98±0.24) in stage I was significantly lower than those in stage II (3.00±0.26) and III (4.12±0.41) ($P < 0.05$). The air trapping score (0.35±0.10) of inspiratory phase of chest CT was lower in stage I than that in stage IV (1.5±0.76) ($P < 0.05$) (Table-3). The GGO score was higher than consolidation, fibrosis and air trapping scores of all the patients, however, there was no significant difference of GGO score among CT stages ($P > 0.05$).

2. Correlation analysis

There were significant correlations among the ABG analysis indices - PaO2, SpO2 and OI, as well as among the CT scores of GGO, consolidation, fibrosis and air trapping. However, there were no correlations between the ABG analysis indices and CT scores ($P > 0.05$), except the weak relevance between the fibrosis score and PaO2 ($P=0.017$, $r=0.218$) and between fibrosis score and SpO2 ($P=0.032$, $r=0.206$), as showed in Table-4.

**Discussion**

The SARS-CoV-2 infection is recognized as a global health hazard. The disease is highly infectious. It is suspected that infection is transmitted by means of large-particle respiratory droplets produced by coughing or touch contamination; hence, good respiratory and hand hygiene is important[8].

A greater number of men (58.1%, 136/234) was found than that of women (41.9%, 98/234), which was similar to previous studies[9]. The reduced susceptibility of females to viral infections might be attributed to the protection from X chromosome and sex hormones, which play an important role in innate and adaptive immunity[10]. Almost 90% patients in present study were classified as common type. Fever and cough were main symptoms. However, some patients presented initially with atypical symptoms, such as diarrhea, nausea and vomiting. A large proportion of patients was with normal blood routine examination. Up to February 18, 2020, a total of 629 COVID-19 confirmed cases have been reported without death in Jiangsu Province, compared to Hubei Province 59989 cases with 1789 death. Most cases in Jiangsu were with mild clinical symptoms and approximately 90% patients had epidemiologic linkage to Hubei Province or closely contacted with other confirmed cases in present study, suggesting that the virus may mutate to produce the first generation, the second generation and so on, with the longer the mutation time, the lower the toxicity, as the MERS-CoV [11][12]. Because of the relatively lower toxicity, clinical symptoms are slight and the prognosis is relatively good.

As SARS-CoV-2 is highly contagious and with a high incidence, early detection is of great importance. Chest HRCT is a critical screening method for COVID-19 due to its high sensitivity and convenience, although 15 patients with COVID-19 were without abnormal lung changes on initial CT images in present study. Additionally, 6 patients were with pneumonia detected by HRCT, but initial RT-PCR was negative with follow-up test positive. These results suggest that both chest HRCT examination and RT-PCR detection of novel coronavirus nucleic acid have limitations which inevitably lead to false-negative. In the follow-up of the initial negative CT cases, pneumonia will be emerged in some patients, while the initial negative RT-PCR cases will be emerged with positive outcomes after redetection for one time or more than once. It suggests the critical importance to combine the two methods in the early stage of the disease to exclude the SARS-CoV-2 infection.

There are some typical findings on CT images. The abnormal attenuations are highly frequently located in bilateral multiple lung lobes and distributed in the lower and/or periphery of the lungs, with the shape of irregular, small patches, strip-like, round-like and “anti-butterfly”. VES was the most frequent sign, followed by interlobular septal thickening, air bronchus sign, intralesional and/or perilesional bronchiectasis, pleural thickening, solid nodules, reticular/mosaic sign, etc. These CT performances of COVID-19 were similar to previous studies[5][13]. In addition, a few cases of mediastinal lymph node enlargement, pleural effusion and pericardial effusion were found in present study, which were not reported yet. It may be due to the relatively small sample size of previous study. Furthermore, there are group differences of some CT signs among different CT stages, though GGOs and VES sign were most frequently seen in each CT stages without group differences in patients with COVID-19 pneumonia. In the early stage, interlobular septal thickening, air bronchus sign, intralesional and/or perilesional bronchiectasis and bronchial wall thickening was less seen than that in progressive stage. The reticular sign, pleural thickening and interlobar fissure displacement was not common in early stage. The frequency of pleural effusion, pericardial effusion and mediastinal lymphadenopathy was relatively small. The quantified evaluation of CT images demonstrated that consolidation, fibrosis and air trapping were minor in the early stage. These results suggest that each CT stage has its characteristic CT signs and performances, making it possible to radiologists and physicians to quickly obtained the stage of the pneumonia.

As to the ABG results, the SpO2 and OI decreased in patients with severe stage than early or progressed stage, which were in consistence with the alteration of indices in patients with severe or critical severe clinical type. In the severe stage of CT, the bilateral diffuse parenchymal abnormalities were mainly GGO lesions, with consolidation, fibrosis and air trapping. It might demonstrate the severity of pulmonary dysfunction caused by SARS-CoV-2 infection. While the fibrosis score was higher in the recovery stage, which might indicate an improvement of the disease. And a weak positive relevance was found between the fibrosis score and ABG indices (PaO2 and SpO2), that was, a patient with higher fibrosis score tended to have better ABG results, suggesting that fibrosis score may be a potential index in the prognosis of the disease.

There were several limitations in this study. First, the patients underwent the CT scans with different machine type, due to the multiple centers in the study. The heterogeneity of the CT data may affect the results of the study. Second, none of the patients underwent a lung biopsy or autopsy, because of the comparatively better outcomes of the patients in this study. Therefore, the CT findings of the lung could not be verified by histopathology. Finally, this was a retrospective study with initial CT images during hospitalization, mainly demonstrated the early pulmonary lesions in patients with COVID-19. A further longitudinal research was needed to focus on the long-term follow-up, to provide dynamic CT evaluation for pulmonary lesions and to obtain the data of long-term pulmonary function changes.

In conclusion, clinical performances of patients with COVID-19, mostly with epidemiologic history and typical symptoms, were critical valuable in the diagnosis of the COVID-19. While chest HRCT provided the distribution, shape, attenuation and extent of lung lesions, as well as some typical CT signs of COVID-19 pneumonia.

.

**Acknowledgments**

This work was mainly supported by the National Natural Science Foundation of China (grant number 81971573, 81671743), the Clinical Key diseases diagnosis and therapy Special project of Health and Family Planning Commission of Suzhou (LCZX201801), the Project of Invigorating Health Care through Science, Technology and Education, Jiangsu Provincial Medical Youth Talent (QNRC2016709), the High-level Health Personnel "six-one" Project of Jiangsu Province (LGY2016035) and Program for Advanced Talents within Six Industries of Jiangsu Province (WSW-057).

**Ethical Approval**

Independent ethics committees approved the protocol, and the approval number was respectively 2020 the 30th, 2020001, 2020 the 2th, KY 202000701, E2020002, 2020ZDSYLL016-P01, 02A-A2020002, 202002, 2020 the 6th, 20200217, 2020-SL-0004.

References

[1] Ksiazek TG, Erdman D, Goldsmith CS, Zaki SR, Peret T, Emery S, Tong S, Urbani C, Comer JA, Lim W, Rollin PE, Dowell SF, Ling AE, Humphrey CD, Shieh WJ, Guarner J, Paddock CD, Rota P, Fields B, DeRisi J, Yang JY, Cox N, Hughes JM, LeDuc JW, Bellini WJ, Anderson LJ; SARS Working Group. A novel coronavirus associated with severe acute respiratory syndrome. N Engl J Med **2003**; 348:1953–66.

[2] K Kuiken T, Fouchier RA, Schutten M, Rimmelzwaan GF, van Amerongen G, van Riel D, Laman JD, de Jong T, van Doornum G, Lim W, Ling AE, Chan PK, Tam JS, Zambon MC, Gopal R, Drosten C, van der Werf S, Escriou N, Manuguerra JC, Stöhr K, Peiris JS, Osterhaus AD. Lancet **2003**; 362:263–70.

[3] de Groot RJ, Baker SC, Baric RS, Brown CS, Drosten C, Enjuanes L, Fouchier RA, Galiano M, Gorbalenya AE, Memish ZA, Perlman S, Poon LL, Snijder EJ, Stephens GM, Woo PC, Zaki AM, Zambon M, Ziebuhr J. Middle East respiratory syndrome coronavirus (MERS-CoV): announcement of the Coronavirus Study Group. J Virol **2013**; 87:7790–92.

[4] Huang C, Wang Y, Li X, Ren L, Zhao J, Hu Y, Zhang L, Fan G, Xu J, Gu X, Cheng Z, Yu T, Xia J, Wei Y, Wu W, Xie X, Yin W, Li H, Liu M, Xiao Y, Gao H, Guo L, Xie J, Wang G, Jiang R, Gao Z, Jin Q, Wang J, Cao B. Clinical features of patients infected with 2019 novel coronavirus in Wuhan, China.Lancet **2020**;395:497-506.

[5] Chung M, Bernheim A, Mei X, Zhang N, Huang M, Zeng X, Cui J, Xu W, Yang Y, Fayad ZA, Jacobi A, Li K, Li S, Shan H. CT Imaging Features of 2019 Novel Coronavirus (COVID-19). Radiology.**2020**;200230. [Preprint]. Available from: https://

doi.org/10.1148/radiol.2020200230.
[6] Yun TJ, Park CM, Kwon GJ, Woo SK, Park SH, Choi SH, Lee HJ, Goo JM. Clinical and radiological features of pandemic H1N1 2009 influenza virus infection manifesting as acute febrile respiratory illness at their initial presentations: comparison with contemporaneous non-H1N1 patients. Acta Radiol **2011**;52:410-416.
[7] Ng CK, Chan JW, Kwan TL, To TS, Chan YH, Ng FY, Mok TY. Six month radiological and physiological outcomes in severe acute respiratory syndrome (SARS) survivors. Thorax **2004**;59:889–91.
[8] Swerdlow DL. Preparation for Possible Sustained Transmission of 2019 Novel Coronavirus: Lessons From Previous Epidemics. JAMA **2020**. [Preprint]. Available from: https://doi.org/10.1001/jama.2020.1960.
[9] Chen N, Zhou M, Dong X, Qu J, Gong F, Han Y, Qiu Y, Wang J, Liu Y, Wei Y, Xia J, Yu T, Zhang X, Zhang L. Epidemiological and clinical characteristics of 99 cases of 2019 novel coronavirus pneumonia in Wuhan, China: a descriptive study. Lancet **2020**;395:507-513.
[10] Jaillon S, Berthenet K, Garlanda C. Sexual dimorphism in innate immunity. Clin Rev Allergy Immunol **2019**; 56:308–21
[11] Poletto C, Colizza V. Quantifying spatiotemporal heterogeneity of MERS-CoV transmission in the Middle East region: A combined modelling approach. Epidemics. **2016**;15:1-9.
[12] Drosten C, Meyer B, Müller MA, Corman VM, Al-Masri M, Hossain R, Madani H, Sieberg A, Bosch BJ, Lattwein E, Alhakeem RF, Assiri AM, Hajomar W, Albarrak AM,

Al-Tawfiq JA, Zumla AI, Memish ZA. Transmission of MERS-coronavirus in household contacts. N Engl J Med .**2014**;371:828-835.

[13] Chest CT Findings in 2019 Novel Coronavirus (2019-nCoV) Infections from Wuhan, China: Key Points for the Radiologist. Radiology **2020**;200241 [Preprint]. Available from:https://doi.org/10.1148/radiol.2020200241.

Table-1 Demographics of 234 patients infected with SARS-CoV-2 in Jiangsu, China

| Items | Sub-items | Case distribution |
|---|---|---|
| Age (years) | 0-9 | 1（0.4%） |
| | 10-19 | 4（1.7%） |
| | 20-29 | 38（16.2%） |
| | 30-39 | 52（22.2%） |
| | 40-49 | 47（20.1%） |
| | 50-59 | 54（23.1%） |
| | 60-69 | 30（12.8%） |
| | 70-79 | 7（3.0%） |
| | 80-89 | 1（0.4%） |
| Gender | Men | 136（58.1%） |
| | Woman | 98（41.9%） |
| Occupation | None | 26（11.1%） |
| | Stuff | 108（46.2%） |
| | Student | 11（4.7%） |
| | Medical staff | 3（1.3%） |
| | Farmer | 26（11.1%） |
| | Others | 60（25.6%） |
| Epidemic history | epidemiologic linkage to Hubei Province | 133（56.8%） |
| | epidemiologic linkage to other confirmed cases, without traveling to Hubei | 78（33.3%） |
| | None | 23（9.8%） |
| Disease severity | Mild | 9 (3.9%) |

| | |
|---|---|
| Common | 210 (89.7%) |
| Severe | 13（5.5%） |
| Critical severe | 2（0.9%） |

Table-2 Comparison of the frequency of HRCT signs among different CT stages

| | I-II | | I-III | | I-IV | | II-III | | II-IV | | III-IV | |
|---|---|---|---|---|---|---|---|---|---|---|---|---|
| | P | χ2 | P | χ2 | P | χ2 | P | χ2 | P | χ2 | P | χ2 |
| VES | 0.051 | 4.312 | 0.303 | 1.071 | 0.298 | 1.098 | 0.474 | 0.516 | 0.628 | 0.238 | 0.491 | 0.483 |
| Air bronchus | 0.000 | 36.033 | 0.001 | 11.118 | 0.018 | 5.625 | 0.025 | 5.098 | 0.733 | 0.118 | 0.320 | 1.006 |
| Reticular sign | 0.000 | 33.007 | 0.001 | 11.837 | 0.000 | 15.395 | 0.151 | 2.078 | 0.110 | 2.576 | 0.037 | 4.425 |
| BWT | 0.273 | 1.209 | 0.001 | 10.999 | 0.002 | 9.256 | 0.016 | 5.895 | 0.016 | 5.837 | 0.347 | 0.900 |
| IST | 0.000 | 16.436 | 0.004 | 8.492 | 0.152 | 2.072 | -- | -- | -- | -- | -- | -- |
| IFD | 0.000 | 48.945 | 0.000 | 32.987 | 0.000 | 26.250 | 0.886 | 0.021 | 0.079 | 3.126 | 0.075 | 3.228 |
| Solid nodules | 0.136 | 2.238 | 0.036 | 4.450 | 0.004 | 8.221 | 0.357 | 0.855 | 0.022 | 5.324 | 0.060 | 3.607 |
| Bronchiectasis* | 0.000 | 25.624 | 0.000 | 20.328 | 0.041 | 4.219 | 0.354 | 0.867 | 0.943 | 0.005 | 0.514 | 0.435 |
| Pleural | 0.000 | 26.495 | 0.000 | 19.657 | 0.005 | 7.854 | 0.522 | 0.413 | 0.285 | 1.155 | 0.394 | 0.740 |
| MI | 0.040 | 4.250 | 0.002 | 9.712 | 0.012 | 6.410 | 0.199 | 1.660 | 0.373 | 0.803 | 0.920 | 0.010 |
| Pleural effusion | 0.014 | 6.081 | 0.000 | 15.763 | 0.000 | 27.960 | 0.070 | 3.315 | 0.003 | 8.930 | 0.133 | 2.295 |
| Pericardial | 0.682 | 0.169 | 0.564 | 0.335 | 0.140 | 2.203 | 0.347 | 0.892 | 0.079 | 3.126 | 0.322 | 0.998 |

Note: VES- Vascular enhancement sign, Bronchiectasis*- intralesional and/or perilesional bronchiectasis, BWS-Bronchial wall thickening, IST-Interlobular septal thickening, IFD- Interlobar fissure displacement, MI- Mediastinal lymphadenopathy; "--" in the row of IST without exact number is due to that IST variable was considered as a constant for the identical component ratio of stage II, III and IV.

Table-3 The group differences of SpO2, OI, and CT scores of consolidation, fibrosis and air trapping

| | I-II | | I-III | | I-IV | | II-III | | II-IV | | III-IV | |
|---|---|---|---|---|---|---|---|---|---|---|---|---|
| | P | Z | P | Z | P | Z | P | Z | P | Z | P | Z |
| SpO2 | 0.846 | -1.472 | 1.000 | 0.071 | 0.083 | 2.463 | 0.806 | 1.497 | 0.008 | 3.200 | 0.096 | 2.408 |
| OI | 0.414 | 1.818 | 0.963 | 1.404 | 0.009 | 3.176 | 1.000 | -0.067 | 0.229 | 2.073 | 0.453 | 1.778 |
| Consolidation | 0.001 | -3.820 | 0.009 | -3.165 | 0.191 | -2.147 | 1.000 | -0.027 | 1.000 | -0.379 | 1.000 | -0.346 |
| Fibrosis | 0.021 | -2.917 | 0.000 | -4.520 | 0.470 | -1.760 | 0.189 | -2.150 | 1.000 | -0.411 | 1.000 | 0.752 |
| Air trapping | 1.000 | -0.737 | 0.544 | -1.692 | 0.045 | -2.675 | 1.000 | -1.100 | 0.115 | -2.343 | 0.601 | -1.644 |

Note: SpO2, oxygen saturation; OI, oxygenation index

Table-4 The correlations between ABG analysis indices and CT scores

| | GGO | | Consolidation | | Fibrosis | | Air trapping | |
|---|---|---|---|---|---|---|---|---|
| | P | r | P | r | P | r | P | r |
| RR | 0.948 | 0.006 | 0.229 | 0.103 | 0.842 | -0.017 | 0.896 | 0.011 |
| PaO2 | 0.459 | 0.068 | 0.202 | 0.118 | 0.017 | 0.218 | 0.118 | 0.144 |
| SpO2 | 0.752 | 0.031 | 0.089 | 0.164 | 0.032 | 0.206 | 0.115 | 0.235 |
| OI | 0.167 | 0.217 | 0.740 | -0.053 | 0.571 | 0.090 | 0.989 | -0.002 |

Note: ABG, arterial blood gas; GGO, ground-glass opacity; RR, respiratory rate; PaO2, partial pressure of oxygen; SpO2, oxygen saturation; OI, oxygenation index

**Figure legends**

**Figure-1 a–c.** A 53-year-old man with COVID-19 in stage I. Chest axial HRCT images a and b show irregular and round-like GGO in bilateral multiple lobes. Coronal reconstruction image c shows VES in the irregular lesion of left upper lung (arrow).

**Figure-2. a-c.** A 56-year-old man with COVID-19 in stage II. Chest HRCT images a-c show multiple "anti-butterfly" -shaped and irregular GGO with reticular sign in bilateral lungs. Axial CT image b shows the displacement of right interlobar fissure (arrow). Bronchial wall thickening in left upper lung (white arrow) and VES (black arrow) in middle lobe of right lung can be seen on coronal reconstruction CT image c. A few fibrosis (linear arrow) can be seen in bilateral lungs on image a and c.

**Figure-3. a, b.** A 43-year-old man with COVID-19 in stage III. Chest HRCT images show that the lesions absorbed with multiple residual fiber stripes in both lungs, mainly in the lower lung lobes.

**Figure-4. a, b.** A 73-year-old man with COVID-19 in stage IV. Chest HRCT images show bilateral diffuse pneumonia with air bronchus sign.

Highlights

1. An outbreak of pneumonia of COVID-19 was recently reported in China, with highly infectious.
2. This was a multi-centered study included 234 inpatients confirmed with COVID-19 from 13 hospitals during 17 days (from January 10th to February 7th 2020) in Jiangsu province. Most of these cases were introduced from Wuhan, and they might have some distinctive clinical and imaging features.
3. The comprehensive chest CT characteristics and clinical features of patients with COVID-19 were described in this study.

**Conflict of interest**

No conflict of interest exits in the submission of this manuscript.

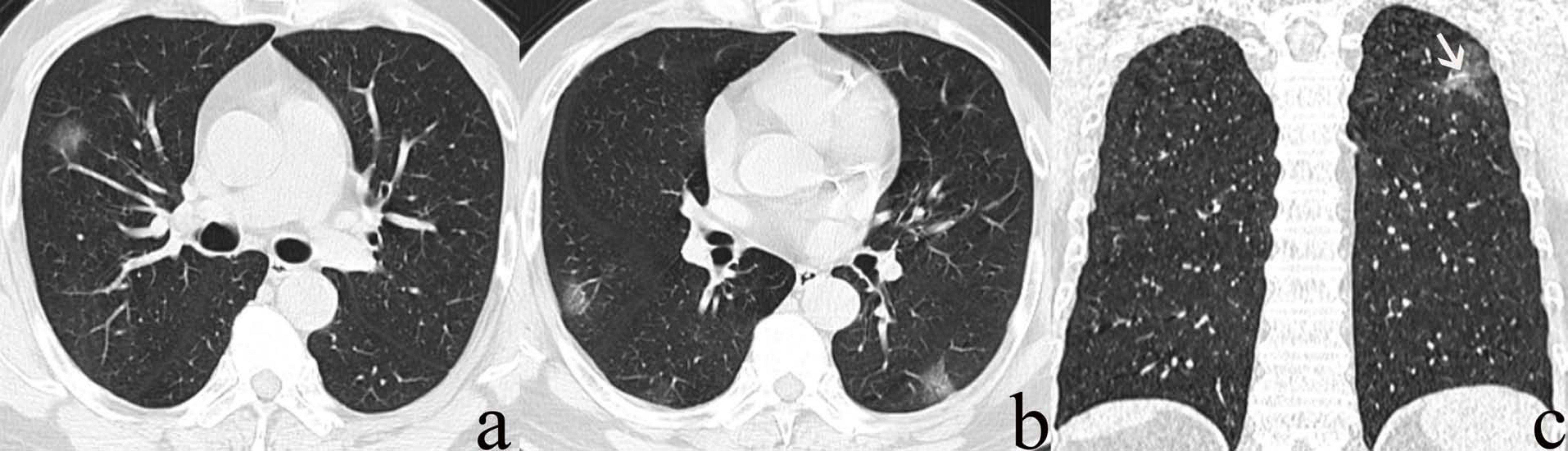
a
b
c

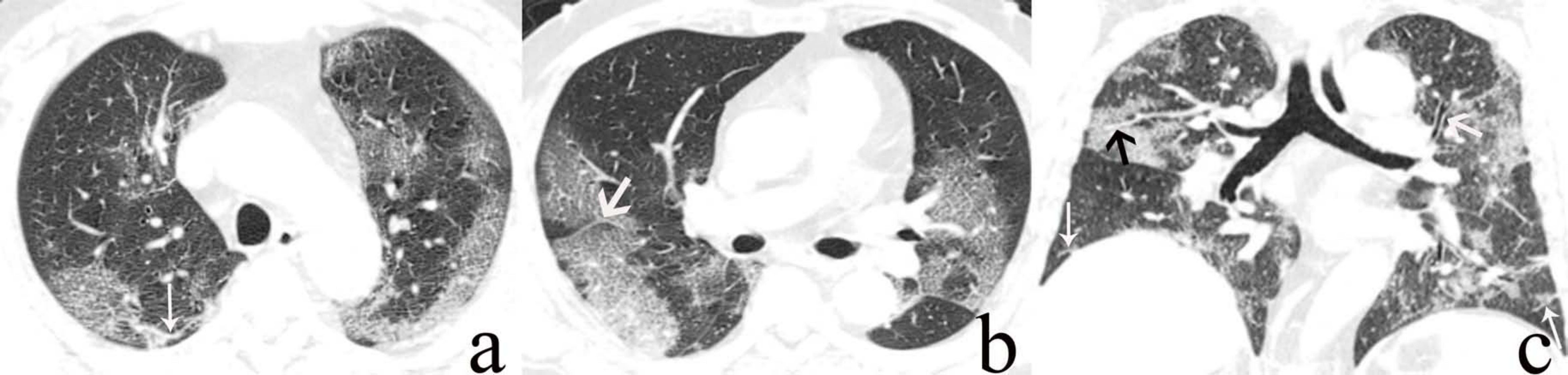
a
b
c

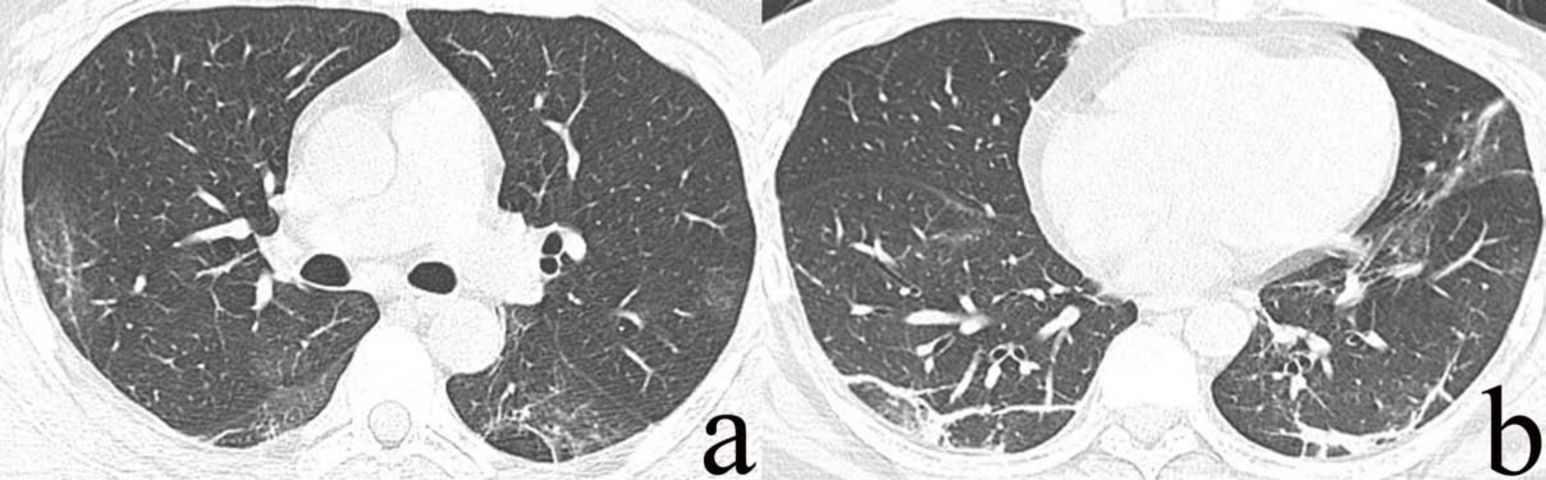
a
b

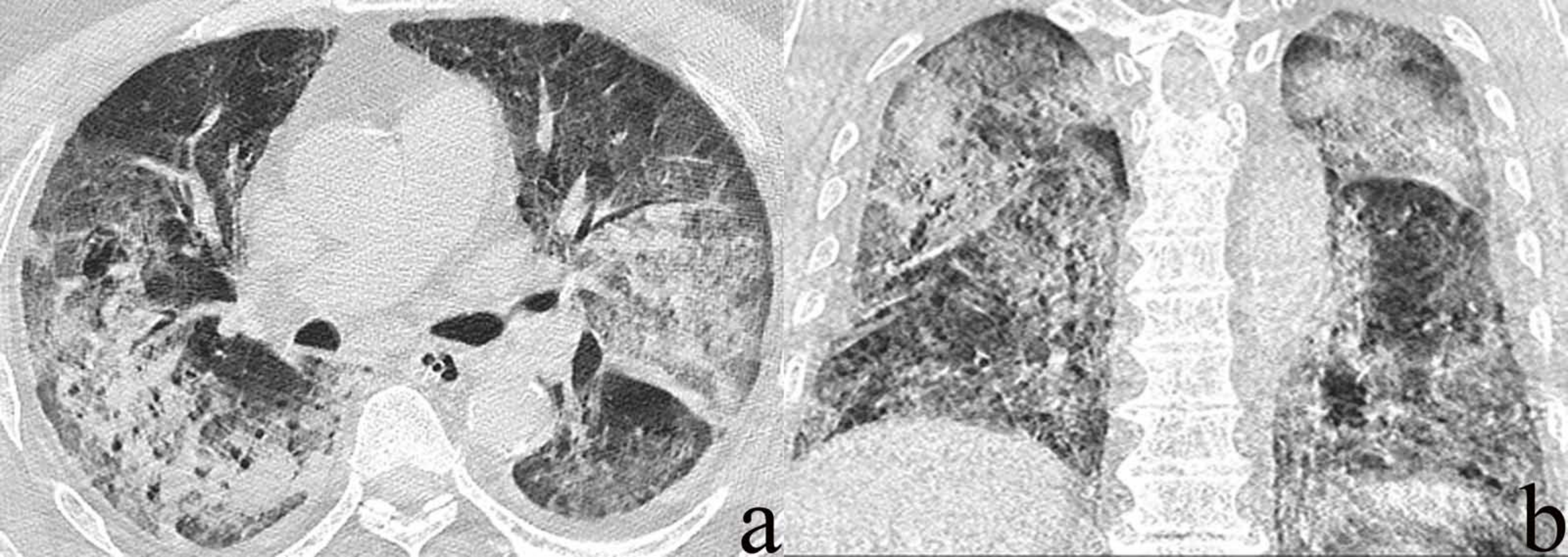
a
b